Medical Molecular Morphology (2019) 52:156–163
https://doi.org/10.1007/s00795-018-0213-z

ORIGINAL PAPER

Fgfr1 conditional-knockout in neural crest cells induces heterotopic chondrogenesis and osteogenesis in mouse frontal bones

Mariko Kawai[1,2] · David Herrmann[2] · Alisa Fuchs[2] · Shuofei Cheng[2] · Anna Ferrer-Vaquer[2] · Rebekka Götz[2] · Katrin Driller[2] · Annette Neubüser[2] · Kiyoshi Ohura[1]

Received: 28 September 2018 / Accepted: 21 November 2018 / Published online: 29 November 2018

Abstract
Most facial bones, including frontal bones, are derived from neural crest cells through intramembranous ossification. Fibroblast growth factor receptor 1 (Fgfr1) plays a pivotal role in craniofacial bone development, and loss of Fgfr1 leads to cleft palate and facial cleft defects in newborn mice. However, the potential role of the *Fgfr1* gene in neural crest cell-mediated craniofacial development remains unclear. To investigate the role of *Fgfr1* in neural crest cells, we analyzed *Wnt1-Cre;Fgfr1*$^{flox/flox}$ mice. Our results show that specific knockout of *Fgfr1* in neural crest cells induced heterotopic chondrogenesis and osteogenesis at the interface of the anterior portions of frontal bones. We observed that heterotopic bone formation continued through postnatal day 28, whereas heterotopic chondrogenesis lasted only through the embryonic period. In summary, our results indicate that loss of *Fgfr1* in neural crest cells leads to heterotopic chondrogenesis and osteogenesis.

Keywords *Fgfr1* · Neural crest cell · Frontal bone · Chondrogenesis · Osteogenesis

Introduction

Most facial bones, including the palatine, maxilla, and pterygoid bones, are derived from neural crest cells [1]. A previous report using Wnt1-Cre transgenic and *ROSA26* conditional reporter (*R26R*) mice [2] showed that frontal bones also originated from neural crest cells through intramembranous ossification.

Fibroblast growth factor receptor 1 (FGFR1) is a member of the vertebrate *Fgfr* gene family, comprising four highly related genes, *Fgfr1–4*, each of which encodes a receptor tyrosine kinase [3]. These receptors have an extracellular ligand-binding domain, a transmembrane region, an alternatively spliced juxtamembrane domain, and an intracellular tyrosine kinase signaling region. *Fgfr1*-knockout embryos have prominent defects during early development caused by aberrant mesodermal migration and patterning, which lead to embryonic lethality during gastrulation [4].

✉ Mariko Kawai
kawai-m@cc.osaka-dent.ac.jp

[1] Department of Pharmacology, Osaka Dental University, 8-1 Kuzuhahanazono-cho, Hirakata, Osaka 573-1121, Japan

[2] Department of Developmental Biology, Institute of Biology I, University of Freiburg, Freiburg, Germany

Because of this early embryonic lethality, a conditional allele of *Fgfr1* was generated by introducing loxP sites into the intronic regions flanking exons 8 and 15 [5, 6]. Cre-mediated recombination then enabled deletion of the sequences encoding the transmembrane and juxtamembrane domains, as well as most of the tyrosine kinase domain. These *Fgfr1-flox* mice were later crossed with mice carrying a transgene expressing Cre recombinase under the *Wnt1* promoter [7]. In these mice, *Cre* was active in neural crest precursors and at the mid-hindbrain boundary, where *Wnt1* was expressed. Therefore, the floxed exons of the *Fgfr1* gene were deleted only in these cells.

Wnt1-Cre;Fgfr1$^{flox/flox}$ mice were previously used to investigate the functions of the *Fgfr1* gene in pharyngeal patterning and at the mid-hindbrain boundary [6], with cleft palate and facial cleft defects observed in these newborn mice. In skeletal preparations, these mice showed open palatine bones and flattened pterygoid bones [6]. However, to date, no complete assessment of craniofacial bone formation has been performed in *Fgfr1* conditional knockout (CKO) *Wnt1-Cre;Fgfr1*$^{flox/flox}$ mice.

In this study, we analyzed cranial bone development in *Wnt1-Cre;Fgfr1*$^{flox/flox}$ mice and *Wnt1-Cre;R26R;Fgfr1*$^{flox/flox}$ mice, which harbored the conditional R26R reporter.

Materials and methods

Mice

*Wnt*1-*Cre*;*Fgfr*1$^{flox/flox}$ mice have been described previously [7]. All experiments were performed in an outbred (129sv/ICR) background. Male *Wnt1-Cre;Fgfr1*$^{flox/+}$ mice and female *Fgfr1*$^{flox/flox}$ mice [7] were mated to yield *Wnt1-Cre;Fgfr1*$^{flox/flox}$ mice. *Fgfr1*$^{flox/flox}$ mice and *Wnt1-Cre;R26R* mice were mated to yield *Wnt1-Cre;R26R;Fgfr1*$^{flox/flox}$ mice. Genotypes were confirmed by polymerase chain reaction (PCR) using tail clips. PCR was performed to detect Cre and the *Fgfr1* wild-type (WT) allele. For Cre-transgenic mice, the forward primer was 5′-CCCACCGTCAGTACGTGA GATATC-3′ and the reverse primer was 5′-CGCGGTCTG GCAGTAAAAACTATC-3′. A 350-bp band was expected. For *Fgfr1*^{flox}, the forward primer was 5′-GAGCTGTAAGCA TAGGCTAG-3′ and the reverse primer was 5′-CTTCTC CCAAAGAGACCTTTC-3′, with a 225-bp band expected for WT alleles but no band if only *Fgfr1*-flox alleles were present. Genotyping of *R26R* mice was conducted as previously reported [2].

Skeletal analysis

Skeletal preparations were made from the heads of E18.5 embryos and from mice at postnatal day 1 (P1), P7, P14, and P28. Embryos at E18.5 derived from *Wnt1-Cre;Fgfr1*$^{flox/flox}$ CKO mice were dissected from the uterus and rinsed in phosphate-buffered saline (PBS). Heads were dissected, skinned, incubated in 100% ethanol for 10 days, and then stained with 0.3% Alcian Blue and 0.1% Alizarin Red in 70% ethanol for cartilage (blue) and ossified tissue containing calcium (red), respectively. The heads were cleared with 2% KOH in 20% glycerol.

Histological analysis

Heads of E16.5 embryos and P10 mice were dissected and fixed with 4% paraformaldehyde in phosphate buffer (pH 7.4). Heads of E16.5 embryos were then directly embedded without decalcification, whereas the heads of P10 mice were decalcified with formic acid for 24 h prior to embedding. Embedded tissues were then cut into 6-µm-thick sections and stained with hematoxylin and eosin (HE) according to standard protocols.

X-gal staining of cryosections

Heads from E16.5 and E18.5 embryos were dissected, embedded in OCT compound, and stored at − 80 °C. Sections (10-µm-thick) were fixed in 0.2% glutaraldehyde/2% paraformaldehyde in PBS and incubated with 1 mg/mL X-Gal staining buffer overnight in the dark at 37 °C. The X-Gal staining buffer consisted of 2 mM $MgCl_2$, 5 mM $K_3Fe(CN)_6$, and 5 mM $K_4Fe(CN)_6$-$3H_2O$ in 1 × PBS. Sections were washed with PBS and counterstained with eosin.

In situ hybridization

We performed in situ hybridization of nonradioactive sections as described previously [8–10]. Briefly, digoxigenin (DIG)-11-UTP-labeled, single-stranded RNA probes were prepared using a DIG RNA-labeling kit (Roche Biochemica). cDNAs for collagen type II (*Col II*), osteopontin (*OPN*), and bone morphogenic protein-4 (*Bmp-4*) were used to generate antisense and sense probes. Hybridization was performed at 55 °C overnight, and wash steps were also performed at the same temperature.

Analysis of bromodeoxyuridine (BrdU) incorporation

Pregnant mice from E15.0 embryos were injected intraperitoneally with BrdU (100 mg/kg body weight) 2 h before the kill. The heads of the embryos (knockout and WT, $n = 3$ per group) were fixed overnight in 4% paraformaldehyde, embedded in paraffin, and sectioned to 5-µm thickness. BrdU was detected immunohistochemically using an anti-BrdU antibody (1:100; GE Healthcare), and sections were then incubated with a biotinylated anti-mouse IgG antibody (1:2000; Vector Laboratories) in blocking buffer with 1.5% horse serum in PBS. Signals were detected using Vectastain ABC (1:2000; Vector Laboratories) in PBS. Sections were counterstained with hematoxylin. We counted the number of BrdU-positive cells in the frontal bone or heterotopic bone area of each section, using three sections for each embryo.

Biochemical tests

Alkaline phosphatase (ALP) activity (IU/mg protein) and calcium (Ca) content (g/mg tissue) were used to quantify frontal bone formation. Frontal bones, except for heterotopic bones from E18.5 embryos of *Wnt1-Cre;Fgfr1*$^{flox/flox}$ ($n = 5$) and WT ($n = 6$) mice derived from the same mother, were weighed and then homogenized in 0.25 M sucrose in a Bio-Mixer Polytron homogenizer. ALP activity and total protein content in the resultant supernatants were determined using the 4-nitrophenyl phosphate method [11]. The sediment was demineralized in 0.5 N hydrochloric acid, and Ca content of the soluble fraction was determined by the *O*-cresolphthalein complex method [12].

Statistical analysis

Results are presented as means ± standard deviations. Statistical analysis of differences between groups (for Ca content and ALP activity) was performed using analysis of variance followed by Fisher's comparison test.

Results

Embryos of *Wnt1-Cre;Fgfr1*$^{flox/flox}$ mice form heterotopic bone and cartilage in the frontal bone

We used the *Wnt1-Cre* system to produce a neural crest-specific knockout of *Fgfr1*. The skulls at E18.5 were morphologically smaller in Fgfr1 CKO mouse embryos ($n=6$) than in WT embryos ($n=5$), and presented marked frontal bone defects (Fig. 1a). Moreover, heterotopic cartilage (Fig. 1a, black arrow) and bone tissue formation (Fig. 1a, white arrow) could be seen in the defective frontal bone, none of which was observed in WT mice. HE staining of the frontal and craniofacial sections of E16.5 embryos ($n=7$) confirmed heterotopic chondrogenesis (Fig. 1b, black arrows) and osteogenesis (Fig. 1b, white arrows). No heterotopic chondrogenesis or osteogenesis was detected in sections from WT embryos ($n=5$).

Serial frontal sections of heads from *Wnt1-Cre;Fgfr1*$^{flox/flox}$ embryos at E16.5 were used for in situ hybridization to examine changes in *Col II, OPN*, and *Bmp-4* expression. We detected strong *Col II* expression in the heterotopic cartilage (Fig. 1c, black arrow) and *OPN* expression in the center of the heterotopic bone (Fig. 1c, white arrow), whereas *Bmp-4* was expressed around the region of heterotopic ossification (Fig. 1c, red arrows).

Minimal calcification is observed in the frontal bones of *Wnt1-Cre;Fgfr1*$^{flox/flox}$ mice

Ca content (0.46 ± 0.23 mg/tissue) and ALP activity (2.73 ± 1.08 IU/mg protein) were significantly lower in the frontal bones of E18.5 *Wnt1-Cre;Fgfr1*$^{flox/flox}$ embryos than in WT embryos (0.79 ± 0.15 mg/tissue and 5.80 ± 1.10 IU/mg protein, respectively; Fig. 1d, e).

Heterotopic cartilage and bone derive from neural crest cells

LacZ-positive cells were used to identify tissues derived from the neural crest cells in *Wnt1-Cre;R26R;Fgfr1*$^{flox/flox}$ mouse tissues. Chondrocytes in the heterotopic cartilage (Fig. 2, black arrows) and cells surrounding the sites of heterotopic ossification (Fig. 2, white arrows) were both lacZ-positive.

Cell proliferation and Col II gene expression are high during early osteogenesis in *Wnt1-Cre;Fgfr1*$^{flox/flox}$ mice

Frontal bone osteogenesis in *Wnt1-Cre;Fgfr1*$^{flox/flox}$ embryos was first observed at E15.0, with *Col II*-expressing cells at the interface between frontal bones (Fig. 3a, black arrow). The same site saw also active cell proliferation, as indicated by positive BrdU staining (Fig. 3a, white arrow). In contrast, only few *Col II*-expressing or actively proliferating cells were detected at the interface of frontal bones in WT mice (Fig. 3a). The number of BrdU-positive cells was generally high at the interface of frontal bones in WT embryos (Fig. 3b) and no significant difference could be seen regarding the total number of cells in frontal bones between WT and *Wnt1-Cre;Fgfr1*$^{flox/flox}$ embryos (Fig. 3b).

Fate of heterotopic cartilage and bone in postnatal Fgfr1 CKO mice

Seven Fgfr1 CKO mouse embryos and five WT embryos were obtained from the same mother. Of the seven *Wnt1-Cre;Fgfr1*$^{flox/flox}$ embryos, five (71.4%) displayed cleft palate at E16.5 and died shortly after birth. The remaining two (28.6%) did not display a cleft palate and survived. All *Wnt1-Cre;Fgfr1*$^{flox/flox}$ mice exhibited heterotopic chondrogenesis and osteogenesis, irrespective of cleft palate, and could be observed postnatally for up to 4 weeks.

Heterotopic cartilage could not be clearly detected in skeletal preparations of postnatal *Wnt1-Cre;Fgfr1*$^{flox/flox}$ mice (Fig. 4a), or by HE staining at P10 (Fig. 4b). However, *Wnt1-Cre;Fgfr1*$^{flox/flox}$ mice manifested heterotopic ossification in skeletal preparations up to P28 (Fig. 4a, white arrow). Heterotopic bone in *Wnt1-Cre;Fgfr1*$^{flox/flox}$ mice had expanded into the interface between the two frontal bones (Fig. 4a, white arrows). In HE staining at P10, heterotopic bone tissue was observed and appeared separated from the original frontal bone tissues (Fig. 4b, arrows).

Discussion

In this study, we analyzed frontal bone formation in *Wnt1-Cre;Fgfr1*$^{flox/flox}$ mice whose *Fgfr1* expression had been knocked-out specifically in neural crest cells. *Fgfr1* knockout led to heterotopic chondrogenesis and osteogenesis in the anterior portion of the frontal bone. Cre activity alone can cause dramatic developmental defects, such as loss of hematopoietic activity and increased apoptosis [13]. We confirmed that Cre activity in *Wnt1-Cre* mice had no effect on the phenotypes observed and described here (data not shown). Therefore, we concluded that this phenotype arose specifically as a result of *Fgfr1* deletion in neural crest cells.

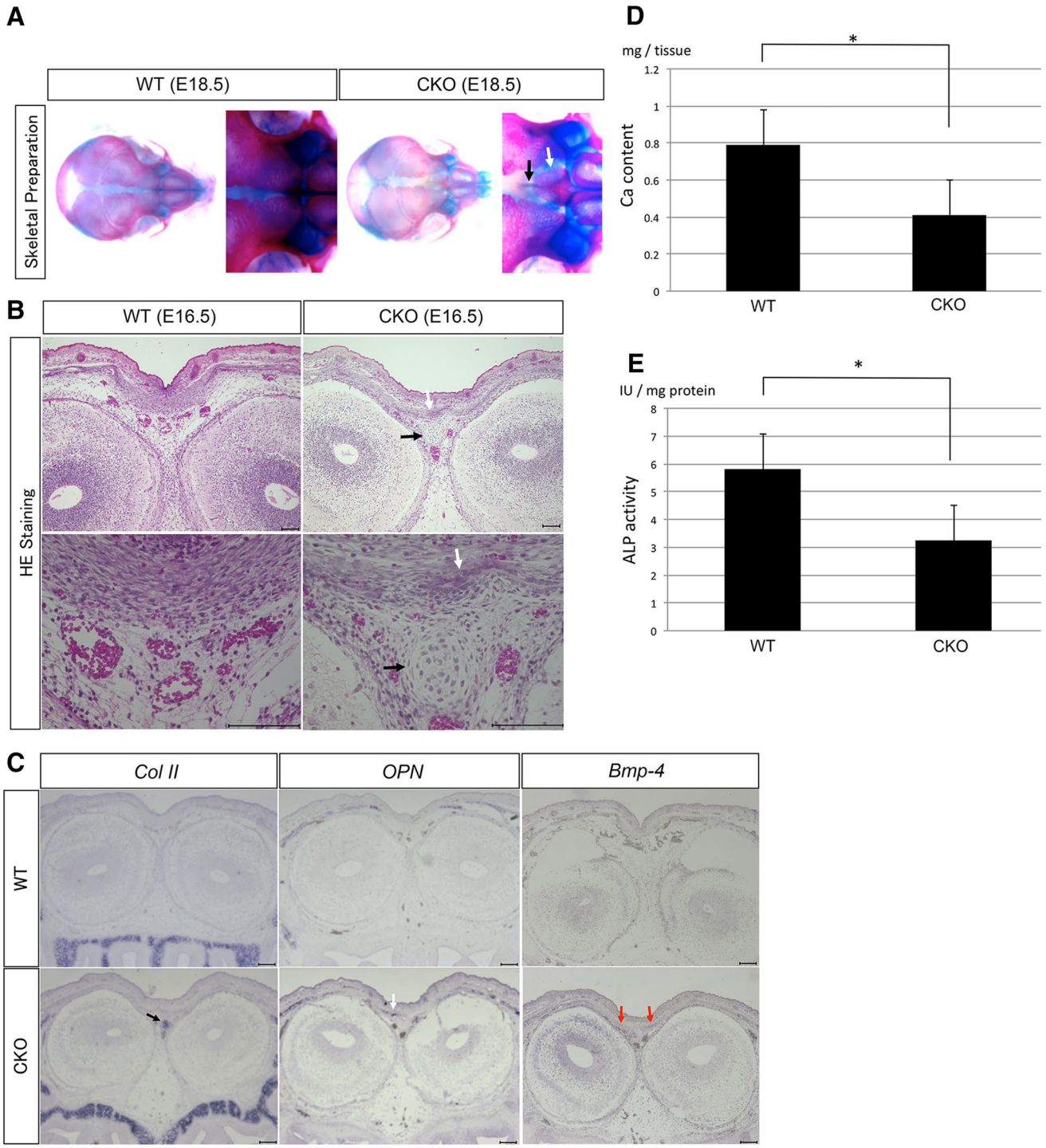

Fig. 1 Phenotype and calcification of frontal bones in *Wnt1-Cre;Fgfr1*$^{flox/flox}$ mice. **a** Skeletal preparations of E18.5 embryos stained with Alcian Blue (cartilage) and Alizarin Red S (bone). Heterotopic chondrogenesis (black arrow) and osteogenesis (white arrow) can be observed among anterior defects of frontal bones in *Wnt1-Cre;Fgfr1*$^{flox/flox}$ mice. Heterotopic chondrogenesis is marked by the formation of a rod-like structure in the anterior–posterior direction. Heterotopic bone is formed above this structure. **b** HE staining of E16.5 embryos showing heterotopic chondrogenesis (black arrows) and osteogenesis (white arrows). **c** *Col II, OPN*, and *Bmp-4* gene expression in the anterior frontal bone of WT and *Wnt1-Cre;Fgfr1*$^{flox/flox}$ mouse embryos at E16.5. *Col II* (black arrow), *OPN* (white arrow), and *Bmp-4* (red arrows) can be observed in the middle of the anterior frontal bone. **d** Ca content and E. ALP activity in frontal bones of WT and *Wnt1-Cre;Fgfr1*$^{flox/flox}$ mouse embryos at E18.5. *CKO* conditional knockout; *WT* wild-type. *$P < 0.05$ for CKO versus WT (unpaired two-tailed *t* test). Scale bars: 100 μm

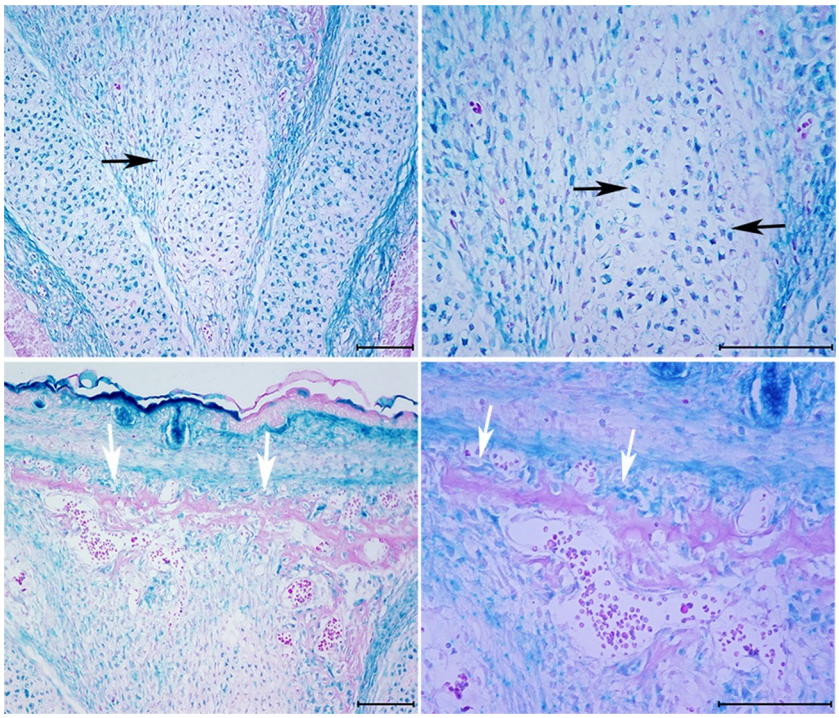

Fig. 2 X-gal staining of *Wnt1-Cre;R26R;Fgfr1*$^{flox/flox}$ mice. X-gal-positive cells can be observed in heterotopic cartilage (black arrows) and heterotopic ossification tissues (white arrows). Magnification: left, ×100; right, ×400. Scale bars: 100 μm

Heterotopic chondrogenesis in *Wnt*1-*Cre*;*Fgfr*1$^{flox/flox}$ mice occurred within the same time frame as normal chondrogenesis in other parts of the skull [14], with specific rod-shaped morphology. Heterotopic ossification occurred also during embryogenesis dorsally to this rod-shaped cartilage. However, we were unable to detect heterotopic chondrogenesis in postnatal skeletal preparations. During craniofacial development, Meckel's cartilage in the mandible disappears in the postnatal stage [15]. Meckel's cartilage is derived from neural crest cells [16] and represents a temporary structure required for subsequent membranous ossification [17, 18]. It is possible that, like Meckel's cartilage, the heterotopic cartilage formed in *Wnt1-Cre;Fgfr1*$^{flox/flox}$ mice acts as a temporary structure for subsequent bone formation. To verify this hypothesis, a more detailed analysis of the fate of heterotopic cartilage, including analysis of apoptosis in *Wnt1-Cre;Fgfr1*$^{flox/flox}$ mice, is required.

*Wnt*1-*Cre*;*Fgfr*1$^{flox/flox}$ embryos displayed heterotopic osteogenesis similar to that observed in mice with conditional deletion of *Msx1* and *Msx2* in neural crest cells [19]. However, in *Msx1*/*Msx2*-deficient mice, heterotopic bone formation was observed at the interface of the posterior portion of the frontal bones and was not accompanied by heterotopic chondrogenesis. The heterotopic osteogenesis observed at the posterior frontal bone was driven by BMP signaling [19]. Although *Bmp-4*-expressing cells were detected in heterotopic bone formed in *Wnt1-Cre;Fgfr1*$^{flox/flox}$ mice, it remains unclear whether ectopic *Bmp-4* expression promoted heterotopic chondrogenesis and/or osteogenesis in this study.

Simultaneous knockout of Axin2 and decreased activity of Fgfr1 in mice has been reported to induce ectopic chondrogenesis in the posterior frontal (PF) and sagittal sutures, leading to abnormal suture morphogenesis and fusion in the postnatal stage [20]. Moreover, *Fgfr1* was inactivated in Axin2-expressing cells and postnatal inactivation of *Fgfr1* led to premature chondrogenesis in the PF suture at P7 in 80% of mice [20]. In contrast, our knockout of *Fgfr1* in the neural crest cells induced ectopic chondrogenesis and osteogenesis in the anterior part of the frontal bone, rather than in the PF suture. Importantly, ectopic chondrogenesis was detected already in the prenatal stage. *In vitro* experiments from the above study indicated that switching the fate of mesenchymal stem cells from an osteoblast progenitor to a chondrocyte progenitor was related to a balance between WNT and FGF signaling [20]. Based on these findings, further studies are required to elucidate the mechanisms mediating cell proliferative activities and heterotopic chondrogenesis in the anterior part of the frontal bone. We also plan to evaluate Axin2 expression in *Wnt1-Cre;Fgfr1*$^{flox/flox}$ mice.

The anterior part of the frontal bone in mice remains unfused at birth [23–23]. In our study, heterotopic cartilage and bone formed at the interface between the two anterior portions of the frontal bones. This heterotopic bone grew towards the posterior frontal bones, with an appearance similar to that of Wormian bones [26–26]. These small bones are often found within sutures and fontanelles of the skull [26–26] and are typically associated with conditions

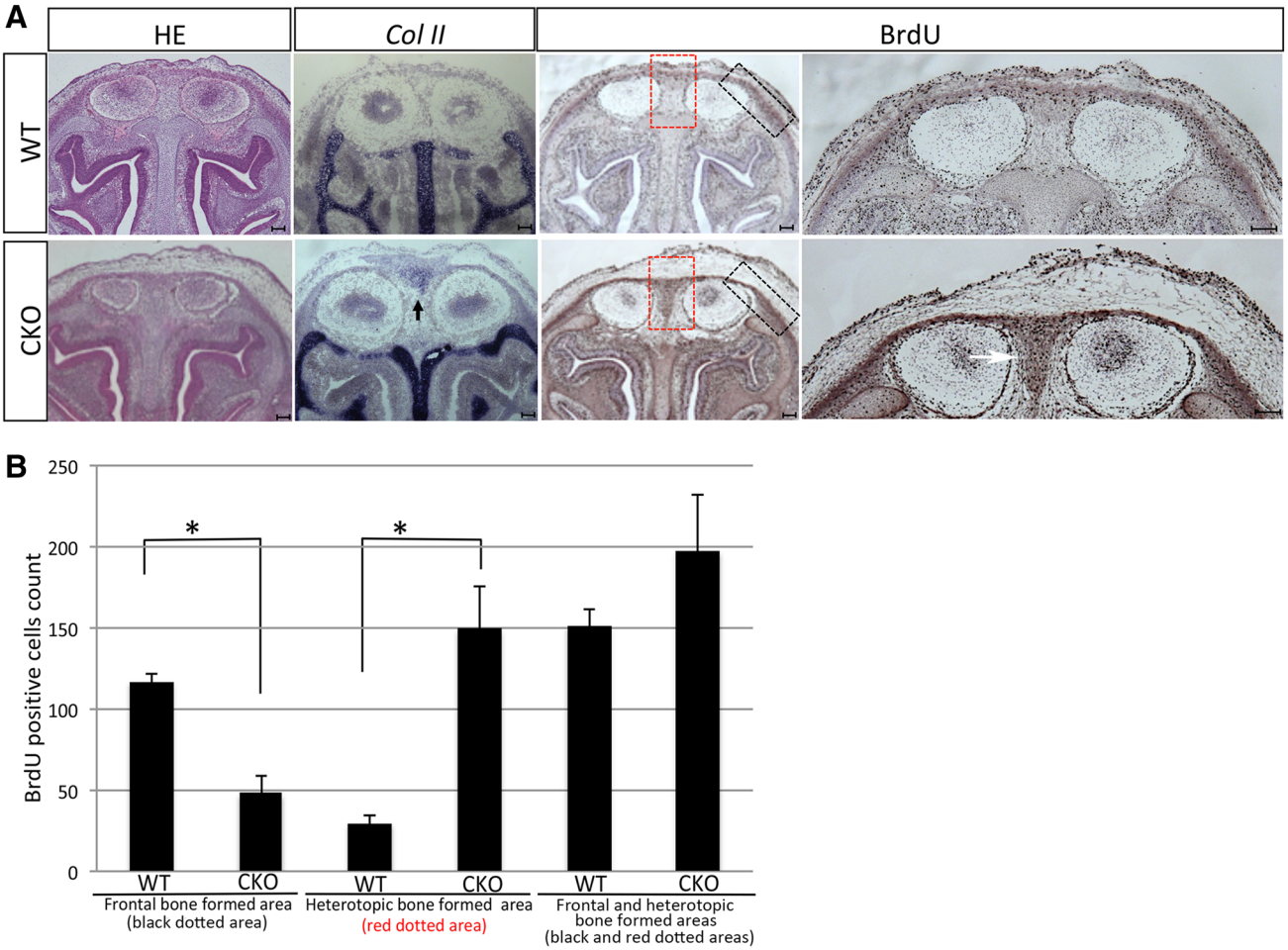

Fig. 3 BrdU and *Col II* gene expression in WT and *Wnt1-Cre;Fgfr1*$^{flox/flox}$ embryos at E15.0. **a** *Col II*-positive cells are visible at the interface of frontal bones during the early stages of osteogenesis (black arrow). BrdU-positive cells (white arrow) are also found in significant numbers at the interface of frontal bones (red dotted area); however, they are fewer in *Wnt1-Cre;Fgfr1*$^{flox/flox}$ than in WT mice. Significant differences in cell proliferation can be seen between *Wnt1-Cre;Fgfr1*$^{flox/flox}$ and WT mice (black dotted area). **b** Total counts of BrdU-positive cells in the frontal bone and heterotopic bone areas in WT and *Wnt1-Cre;Fgfr1*$^{flox/flox}$ mice. *CKO* conditional knockout; *WT* wild-type. *$P < 0.05$ (unpaired two-tailed *t* test). Scale bars: 100 µm

characterized by bony abnormalities, such as shortened stature in patients with osteogenesis imperfecta. *Wnt1-Cre;Fgfr1*$^{flox/flox}$ mice exhibited also lower Ca content and ALP activity in frontal bones than WT mice, as well as fewer proliferative cells. The latter were concentrated at the interface of anterior frontal bones, where heterotopic cartilage and bone had formed. To this end, it should be noted that patients with Wormian bones frequently exhibit haploinsufficiency (nonsense and frameshift) mutations in *COLIA1* [27]; however, a clear link between phenotypic and genotypic manifestations of the disease has not been established yet and could be the focus of future studies.

In conclusion, our results demonstrate that loss of *Fgfr1* in neural crest cells leads to heterotopic chondrogenesis and osteogenesis during frontal bone development.

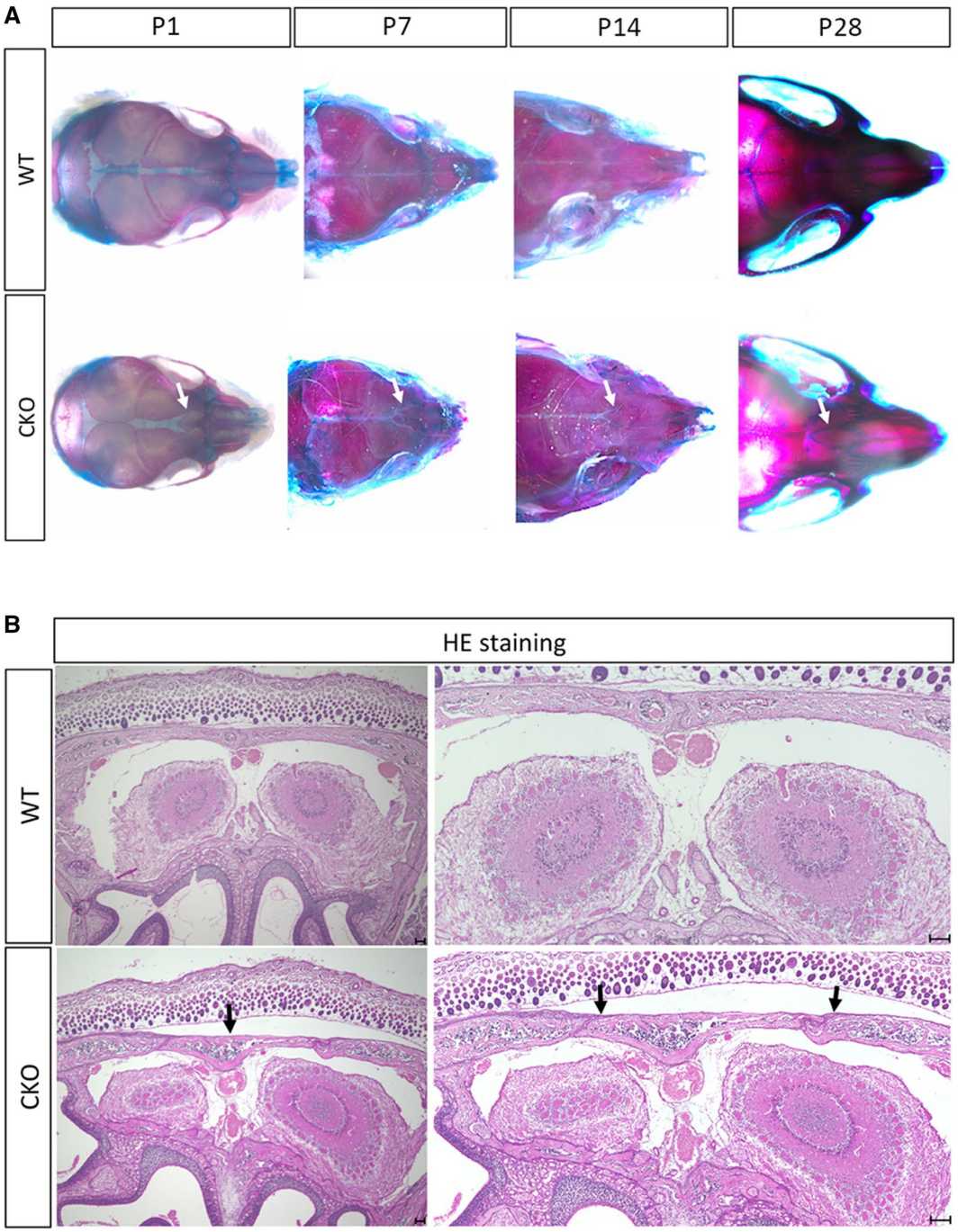

Fig. 4 Fate of heterotopic cartilage and bone in postnatal *Wnt1-Cre;Fgfr1*$^{flox/flox}$ mice. **a** Skeletal preparations of postnatal mice on days 1, 7, 14, and 28. Mouse heads stained with Alcian Blue (cartilage) and Alizarin Red S (bone) show evident ossification but no heterotopic cartilage in *Wnt1-Cre;Fgfr1*$^{flox/flox}$ mice (white arrows). Heterotopic ossification is seen to expand and close the interface between frontal bones up to postnatal day 28 (white arrows). **b** HE staining in sections of frontal bones on postnatal day 10 showing clear evidence of heterotopic bone tissue (black arrows) but no heterotopic cartilage. *CKO* conditional knockout; *WT* wild-type. Scale bars: 100 µm

Acknowledgements We thank Dr. Wolfgang Driever and his laboratory at Freiburg University. This study was supported by Grants-in-Aid for Scientific Research from the Japan Society for the Promotion of Science (Basic Research C Number 24300182) and Nakatomi Foundation.

Compliance with ethical standards

Conflict of interest The authors declare that they have no conflicts of interest.

References

1. Le Lievre CS (1978) Participation of neural crest-derived cells in the genesis of the skull in birds. J Embryol Exp Morphol 47:17–37
2. Jiang X, Iseki S, Maxson RE, Sucov HM, Morriss-Kay GM (2002) Tissue origins and interactions in the mammalian skull vault. Dev Biol 241:106–116
3. Moosa S, Wollnik B (2016) Altered FGF signalling in congenital craniofacial and skeletal disorders. Semin Cell Dev Biol 53:115–125
4. Yamaguchi TP, Harpal K, Henkemeyer M, Rossant J (1994) Fgfr-1 is required for embryonic growth and mesodermal patterning during mouse gastrulation. Genes Dev 15:3032–3044
5. Trokovic N, Trokovic R, Mai P, Partanen J (2003) Fgfr1 regulates patterning of the pharyngeal region. Genes Dev 17:141–153
6. Trokovic R, Trokovic N, Hernesniemi S, Pirvola U, Weisenhorn DM, Rossant J, McMahon AP, Wurst W, Partanen J (2003) FGFR1 is independently required in both developing mid- and hindbrain for sustained response to isthmic signals. EMBO J 22:1811–1823
7. Danielian PS, Muccino D, Rowitch DH, Michael SH, McMahon AP (1998) Modification of gene activity in mouse embryos in utero by a tamoxifen-inducible form of Cre recombinase. Curr Biol 8:1323–1326
8. Adams JC (1992) Biotin amplification of biotin and horseradish peroxidase signals in histochemical stains. J Histochem Cytochem 40:1457–1463
9. Shibata S, Fujimori T, Yamashita Y (2006) An in situ hybridization and histochemical study of development and postnatal changes of mouse mandibular angular cartilage compared with condylar cartilage. J Med Dent Sci 53:41–50
10. Yamamoto H, Ito K, Kawai M, Murakami Y, Bessho K, Ito Y (2006) RunX3 expression during mouse tongue and palate development. Anat Rec A Discov Mol Cell Evol Biol 288:695–699
11. Okubo Y, Bessho K, Fujimura K, Iizuka T, Miyatake S (1999) Osteoinduction by bone morphogenetic protein-2 via adenoviral vector in C2C12 myoblasts induces differentiation in to the osteoblast lineage. Biochem Biophys Res Commun 267:382–387
12. Connery HV, Briggs AR (1966) Determination of serum calcium by means of orthocresolphthalein complex one. Am J Clin Pathol 45:290–296
13. Naiche LA, Papaioannou VE (2007) Cre activity causes widespread apoptosis and lethal anemia during embryonic development. Genesis 45:768–775
14. Kobayashi T, Kronenberg HM (2014) Overview of skeletal development. Methods Mol Biol 1130:3–12
15. Parada C, Chai Y (2015) Mandible and tongue development. Curr Top Dev Biol 115:31–58
16. Chai Y, Jiang X, Ito Y, Bringas PJ, Han J, Rowitch DH, Soriano P, McMahon AP, Sucov HM (2000) Fate of the mammalian cranial neural crest during tooth and mandibular morphogenesis. Development 127:1671–1679
17. Sakakura Y, Tsuruga E, Irie K, Hosokawa Y, Nakamura H, Yajima T (2005) Immunolocalization of receptor activator of nuclear factor-kappaB ligand (RANKL)and osteoprotegerin (OPG) in Meckel's cartilage compared with developing endochondral bones in mice. J Anat 207:325–337
18. Sakakura Y, Hosokawa Y, Tsuruga E, Irie K, Yajima T (2007) *In situ* localization of gelatinolytic activity during development and resorption of Mechel's cartilage in mice. Eur J Oral Sci 115:212–223
19. Roybal PG, Wu NL, Sun J, Ting MC, Schafer CA, Maxson RE (2010) Inactivation of Msx1 and Msx2 in neural crest reveals an unexpected role in suppressing heterotopic bone formation in the head. Dev Biol 34:328–339
20. Maruyama T, Mirando AJ, Deng CX, Hsu W (2010) The balance of WNT and FGF signaling influences mesenchymal stem cell fate during skeletal development. Sci Signal 3(123):ra40. https://doi.org/10.1126/scisignal.2000727
21. Kim HJ, Rice DP, Kethunen PJ, Thesleff I (1998) FGF-, BMP- and Shh-mediated signalling pathways in the regulation of cranial suture morphogenesis and calvarial bone development. Development 12587:1241–1251
22. Rice DP, Aberg T, Chan Y, Tang Z, Kettunen PJ, Pakarinen L, Maxson RE, Thesleff I (2000) Integration of FGF and TWIST in calvarial bone and suture development. Development 127:1845–1855
23. Sahar DE, Longaker MT, Quarto N (2005) Sox9 neural crest determinant gene controls patterning and closure of the posterior frontal cranial suture. Dev Biol 280:344–361
24. Sanches-Lara PA, Graham JMJ, HIng AV, Lee J, Cunningham M (2007) The morphogenesis of wormian bones: a study of craniosynostosis and purposeful cranial deformation. Am J Med Genet A 143:3243–3251
25. Marti B, Sininelli D, Maurin L, Carpentier E (2013) Wormian bones in a general peadiatric population. Diagn Interv Imaging 94:428–432
26. Bellary SS, Steinberg A, Mirzayan N, Shiral M, Tubbs RS, Cohen-Gadol AA, Loukas M (2013) Wormian bones: a review. Clin Anat 26:922–927
27. Semler O, Cheung MS, Glorieux FH, Rauch F (2010) Wormian bones in osteogenesis imperfecta: correlation to clinical findings and genetype. Am J Med Genet A152:1681–1688